Probing photonic content of the proton using photon-induced dilepton production in $p+\mathrm{Pb}$ collisions at the LHC

M. Dyndal and A. Glazov

DESY

M. Luszczak and R. Sadykov

.

Abstract

We propose a new experimental method to validate photon parton distribution function (PDF) inside the proton at LHC energies. It is based on the measurement of dilepton production from the $\gamma p \to \ell^+\ell^- + X$ reaction in proton–lead collisions. These experimental conditions guarantee relatively clean environment, both in terms of reconstruction of the final state and in terms of possible background. We firstly calculate the cross sections for this process with collinear photon PDFs, where we identify correct choice of the scale, in analogy to deep inelastic scattering kinematics. We then include the virtuality of probed photon in the calculations, based on modern parameterizations of deep inelastic structure functions. Finally, we find that significant rates of this process are accessible by LHC experiments with existing datasets.

I. INTRODUCTION

Precise calculations of various electroweak reactions in pp collisions at the LHC need to account for, on top of the higher-order corrections, the effects of photon-induced subprocesses. The relevant examples are the production of lepton pairs [1–5] or pairs of electroweak bosons [6–13].

Recently, a precise photon distribution inside the proton has been evaluated in Ref. [14]. This approach provides a model-independent determination of the photon PDF (embedded in so-called LUXqed distribution) and it is based on proton structure function and elastic form factor fits in electron–proton scattering.

Up to date, there are no experimentally clean processes identified that would allow to either strongly constrain or verify the calculations. For example, the extraction of photon PDF from isolated photon production in deep inelastic scattering (DIS) [15] or from inclusive $pp \to \ell^+\ell^- + X$ reaction [2, 16, 17] is limited due to large QCD background. On contrary, the elastic part of the photon PDF is verified via exclusive $\gamma\gamma \to \ell^+\ell^-$ process, measured in pp collisions by ATLAS [18, 19], CMS [20, 21] and recently by CMS+TOTEM [22] collaborations.

We therefore propose a new experimental method to constrain photonic content of the proton. Thanks to the large fluxes of quasi-real photons from the Pb ion at the LHC, the photon-induced dilepton production in p + Pb collision configuration is a very clean way to probe photon PDF. This process is shown schematically in Fig. 1, where by analogy to DIS, two leading-order diagrams can be identified. Since the photon flux from the ion scales with Z^2 and QCD-induced cross-sections scale approximately with A, the amount of QCD background is greatly reduced comparing to pp case.

Moreover, as this process does not involve the exchange of color with the photon-emitting nucleus, no significant particle production is expected in the rapidity region between the dilepton system and the nucleus. The photon-emitting nucleus is also expected to produce no neutrons because the photons couple to the entire nucleus. Thus, a combination of a rapidity gap and zero neutrons in the same direction provide straightforward criteria to identify these events experimentally.

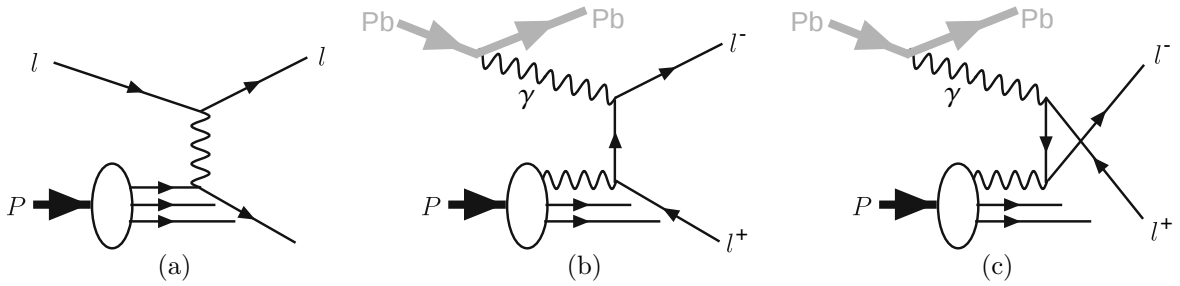

FIG. 1: Schematic graphs for deep inelastic scattering, $\ell^{\pm}p \to \ell^{\pm} + X$ (a) and photon-induced dilepton prodcution, $\gamma p \to \ell^{+}\ell^{-} + X$, in $p+\mathrm{Pb}$ collisions for t-channel (b) and u-channel (c) lepton exchange.

II. FORMALISM

A. Elastic photon fluxes

To get the distribution of the elastic photons from the proton, one can express the equivalent photon flux through the electric and magnetic form factors $G_E(Q^2)$ and $G_M(Q^2)$ of the proton. This contribution is obtained as

$$\gamma_{el}^{p}(x,Q^2) = \frac{\alpha_{\mathrm{em}}}{\pi}\left[\left(1-\frac{x}{2}\right)^2 \frac{4m_p^2 G_E^2(Q^2) + Q^2 G_M^2(Q^2)}{4m_p^2+Q^2} + \frac{x^2}{4} G_M^2(Q^2)\right] , \tag{1}$$

where x is the momentum fraction of the proton taken by the photon, Q^2 is the photon virtuality, α_{em} is the electromagnetic structure constant and m_p is the proton mass.

To express the elastic photon flux for the nucleus ($\gamma_{el}^{\mathrm{Pb}}$), we follow Ref. [23] and replace

$$\frac{4m_p^2 G_E^2(Q^2) + Q^2 G_M^2(Q^2)}{4m_p^2+Q^2} \longrightarrow Z^2 F_{\mathrm{em}}^2(Q^2) , \tag{2}$$

where $F_{\mathrm{em}}(Q^2)$ is the electromagnetic formfactor of the nucleus and Z is its charge. We also neglect the magnetic formfactor of the ion in the following (it even rigorously vanishes for spinless nuclei).

For the Pb nucleus, we use the formfactor parameterization from the STARlight MC generator [24]:

$$F_{\mathrm{em}}(Q^2) = \frac{3}{(QR_A)^3}\Big[\sin(QR_A) - QR_A\cos(QR_A)\Big]\frac{1}{1+a^2Q^2} , \tag{3}$$

where $R_A = 1.1A^{1/3}$ fm, $a = 0.7$ fm and $Q = \sqrt{Q^2}$.

B. Collinear-factorization approach and choice of the scale

The inelastic processes, with breakup of a proton, can be also considered. At LO and at a given scale μ^2, the photon parton distribution $\gamma^p_{inel}(x,\mu^2)$ of photons carrying a fraction z of the proton's momentum, obeys the DGLAP equation:

$$\frac{d\gamma^p_{inel}(x,\mu^2)}{d\log\mu^2} = \frac{\alpha_{\rm em}}{2\pi}\int_x^1 \frac{dy}{y}\Big[\sum_q e_q^2 P_{\gamma\leftarrow q}(y) q\Big(\frac{x}{y},\mu^2\Big) + P_{\gamma\leftarrow\gamma}(y)\gamma^p_{inel}\Big(\frac{x}{y},\mu^2\Big)\Big] , \quad (4)$$

where $q(x,\mu^2)$ is the quark PDF, e_q is the quark charge, $P_{\gamma\leftarrow q}$ is the $q\to\gamma$ splitting function, and $P_{\gamma\leftarrow\gamma}$ corresponds to the virtual self-energy correction to the photon propagator. This is the basis for collinear photon-PDF determination in all initial [25, 26] and more recent [14, 16, 17, 27–30] considerations.

However, none of these studies identify the prescription for the choice of the scale μ^2, which is needed to calculate the cross section for the process of interest. The usual choice for μ is the mass of the system from hard interaction, or the transverse momentum of the leading object. By analogy to DIS (Fig. 1), where the scale is associated with the virtuality of the exchanged photon, it is possible to define the scale in case of the $\gamma\gamma\to\ell^+\ell^-$ process. This is achieved by taking the virtuality of massive t- or u-channel propagator (Fig. 1b or c). Hence, $\mu = p_T^{\ell^-}$ for t-channel diagram and $\mu = p_T^{\ell^+}$ for t-channel exchange. One should note, however, that t/u channel diagrams cannot be separated experimentally. In this case, on can use the average p_T of the leptons with appropriate uncertainty.

In the collinear approach the $p + {\rm Pb} \to {\rm Pb} + \ell^+\ell^- + X$ production cross section can be written as:

$$\sigma = S^2 \int dx_p dx_{\rm Pb}\Big[\big(\gamma^p_{el}(x_p) + \gamma^p_{inel}(x_p,\mu^2)\big)\,\gamma^{\rm Pb}_{el}(x_{\rm Pb})\overline{|\mathcal{M}_{\gamma\gamma\to\ell^+\ell^-}|^2}\Big] , \quad (5)$$

where $\mathcal{M}_{\gamma\gamma\to\ell^+\ell^-}$ is the elementary amplitude for the $\gamma\gamma\to\ell^+\ell^-$ subprocess and S^2 is the so-called survival factor which takes into account the requirement that there be no hadronic interactions between the proton and the ion.

C. k_T-factorization approach

In this approach we start from the Feynman diagrams shown in Fig.**??**, and exploit the high-energy kinematics. Let the four-momenta of incoming protons be denoted p_A, p_B. At

high energies the proton masses can be neglected, so that $p_A^2 = p_B^2 = 0$, $2(p_A \cdot p_B) = s$.

The photon-fusion production mechanism in leptonic and hadronic reactions is in great detail reviewed in [23], where also many original references can be found. In the most general form, the invariant cross section is written as a convolution of density matrices of photons in the beam particles, and helicity amplitudes for the $\gamma^*\gamma^* \to l^+l^-$ process. In a high energy limit, where dileptons carry only a small fraction of the total center-of-mass energy, the density-matrix structure can be very much simplified, and there emerges a k_T-factorization representation of the cross section [31].

The unintegrated photon fluxes introduced in [31] can be expressed in terms of the hadronic tensor as

$$\mathcal{F}^{\rm in.el}_{\gamma^*\leftarrow A}(z,\boldsymbol{q}) = \frac{\alpha_{\rm em}}{\pi}\,(1-z)\left(\frac{\boldsymbol{q}^2}{\boldsymbol{q}^2 + z(M_X^2 - m_A^2) + z^2 m_A^2}\right)^2 \cdot \frac{p_B^\mu p_B^\nu}{s^2}\,W^{\rm in,el}_{\mu\nu}(M_X^2, Q^2) dM_X^2\,. \tag{6}$$

These unintegrated fluxes enter the cross section for dilepton production as

$$\frac{d\sigma^{(i,j)}}{dy_1 dy_2 d^2\boldsymbol{p}_1 d^2\boldsymbol{p}_2} = \int \frac{d^2\boldsymbol{q}_1}{\pi \boldsymbol{q}_1^2}\frac{d^2\boldsymbol{q}_2}{\pi \boldsymbol{q}_2^2}\mathcal{F}^{(i)}_{\gamma^*/A}(x_1,\boldsymbol{q}_1)\,\mathcal{F}^{(j)}_{\gamma^*/B}(x_2,\boldsymbol{q}_2)\frac{d\sigma^*(p_1,p_2;\boldsymbol{q}_1,\boldsymbol{q}_2)}{dy_1 dy_2 d^2\boldsymbol{p}_1 d^2\boldsymbol{p}_2}\,, \tag{7}$$

where the indices $i, j \in \{\rm el, in\}$ denote elastic or inelastic final states. The longitudinal momentum fractions of photons are obtained from the rapidities and transverse momenta of final state leptons as:

$$\begin{aligned} x_1 &= \sqrt{\frac{\boldsymbol{p}_1^2 + m_l^2}{s}}e^{y_1} + \sqrt{\frac{\boldsymbol{p}_2^2 + m_l^2}{s}}e^{y_2}\,, \\ x_2 &= \sqrt{\frac{\boldsymbol{p}_1^2 + m_l^2}{s}}e^{-y_1} + \sqrt{\frac{\boldsymbol{p}_2^2 + m_l^2}{s}}e^{-y_2}\,. \end{aligned} \tag{8}$$

The explicit form of the off-shell cross section $d\sigma^*(p_1,p_2;\boldsymbol{q}_1,\boldsymbol{q}_2)/dy_1 dy_2 d^2\boldsymbol{p}_1 d^2\boldsymbol{p}_2$ can be found in Refs. [4, 31].

D. Structure functions as input for unintegrated fluxes

The different parametrizations taken from the literature are labeled as:

- ALLM [32, 33]: This parametrization gives a very good fit to F_2 in most of the measured region.

- FJLLM [34]: This parametrization explicitly includes the nucleon resonances and gives an excellent fit of the CLAS data.

- SY [35]: This paramerization of Suri and Yennie from the early 1970's does not include QCD-DGLAP evolution. It is still today often used as one of the defaults in the LPAIR event generator.

- SU [36]: A parametrization which concentrates to give a good description at smallish and intermediate Q^2 at not too small x. A Vector-Meson-Dominance model inspired fit of F_2 at low Q^2, which is completed by the same NNLO MSTW structure function as above at large Q^2.

- LUX-like: a newly constructed parametrization, which at $Q^2 > 9\,\mathrm{GeV}^2$ uses an NNLO calculation of F_2 and F_L from NNLO MSTW 2008 partons [**?**]. It employs a useful code by the MSTW group [**?**] to calculate structure functions. At $Q^2 > 9\,\mathrm{GeV}^2$ this fit uses the parametrization of Bosted and Christy [37] in the resonance region, and a version of the ALLM fit published by the HERMES Collaboration [38] for the continuum region. It also uses information on the longitudinal structure function from SLAC [39]. As the fit is constructed closely following the LUXqed work Ref.[40].

III. EXAMPLE EXPERIMENTAL CONFIGURATION AND POSSIBLE BACKGROUND SOURCES

We assume collision setup from recent $p+\mathrm{Pb}$ run at the LHC, carried out at the centre-of-mass energy per nucleon pair $\sqrt{s_{NN}} = 8.16$ TeV. Since the energy per nucleon in the proton beam is larger than in the lead beam, the nucleon–nucleon centre-of-mass system has a rapidity in the laboratory frame of $+0.465$.

As an example of method's applicability, we will use the geometry of ATLAS [41] and CMS [42] detectors in the following. We also consider dimuon-channel only, however the integrated results for ee and $\mu\mu$ channels can be obtained by simply multiplying all cross-sections by a factor of two.

We start with applying minimum transverse momentum requirement of 4 GeV to both muons. This requirement is imposed to ensure high lepton reconstruction and triggering efficiency. Moreover, due to limited acceptance of the detectors, each muon is required to

Variable	Requirement
lepton transverse momentum, p_{T}^{ℓ}	> 4 GeV
lepton pseudorapidity, $\lvert\eta^{\ell}\rvert$	< 2.4
dilepton invariant mass, $m_{\ell^+\ell^-}$	> 10 GeV

TABLE I: Definition of the fiducial region used in the studies.

have a pseudorapidity (η^{ℓ}) that satisfies $|\eta^{\ell}| < 2.4$ condition. Our calculations are carried out for a minimum dilepton invariant mass of $m_{\ell^+\ell^-} = 10$ GeV. Such a choice is due to removal of possible contamination from $\Upsilon(\to \ell^+\ell^-)$ photoproduction process. Summary of all selection requirements is presented in Table I

Possible background for this process can arise from inclusive lepton-pair production, e.g. from Drell–Yan process [43–46]. This processes would lead to disintegration of the incoming ion, and zero-degree calorimeters (ZDC) [47, 48] can be used to veto very-forward-going neutral fragments which would allow to fully reduce this background. Another background can arise from diffractive interactions, hence possibly mimicking signal topology. However, since the nucleus is a fragile object (with the nucleon binding energy of just 8 MeV) even the softest diffractive interaction will likely result in the emission of a few nucleons from the ion, detectable in the ZDC.

Another background category is the photon-induced process with resolved photon, i.e. $\gamma p \to Z/\gamma^* + X$ reaction. Here, the rapidity gap is expected to be smaller than in the signal process due to the additional particle production associated with the "photon remnant". Any other residual contamination of this process can be controlled using dedicated region, with a dilepton invariant mass around the Z-boson mass.

IV. RESULTS WITH COLLINEAR PHOTON-PDFS

We start with the calculation of the elastic contribution, $p + \mathrm{Pb} \to p + \mathrm{Pb} + \ell^+\ell^-$. In this case the photon flux becomes:

$$\gamma_{el}^{p}(x, Q^2) = \gamma_{el}^{p}(x) \tag{9}$$

and the following parameterization is used [23]:

$$\gamma_{el}^{p}(x) = \frac{\alpha_{\rm em}}{\pi}\left(\frac{1-x+0.5x^2}{x}\right)\left(\frac{A+3}{A-1}\log A - \frac{17}{6} - \frac{4}{3A} + \frac{1}{6A^2}\right) , \tag{10}$$

where $A = 1 + \frac{Q_0^2(1-x)}{x m_p^2}$ and $Q_0^2 = 0.71$ GeV^2. This parameterization is a good analytical approximation of Eq. 1 integrated over Q^2.

The results for the elastic case are cross-checked with the calculation from STARlight MC and a good agreement between the fiducial cross-sections is found: $\sigma_{fid}^{\rm el} = 17.5$ nb, whereas $\sigma_{fid}^{\rm STARlight} = 17.0$ nb. Both calculations are also corrected by a factor $S^2 = 0.96$ which is calculated using STARlight, where the hard-sphere proton–nucleus requirement [24] is used.

Next, for the inelastic case ($\gamma p \to \ell^+\ell^- + X$), several recent parameterizations of the photon parton distributions are studied: CT14qed [15], HKR16qed [29], LUXqed17 [40] and NNPDF3.1luxQED [30]. One should note that all of these PDF sets include both elastic and inelastic parts of the photon spectrum. All predictions are scaled by $S^2 = 0.95$, again derived from STARlight. Comparison of several lepton kinematic distributions between different photon-PDFs is shown in Fig. 2.

The integrated fiducial cross-sections are summarized in Tab. II.

(some discussion here...)

It should be made clear, that the calculations with collinear photons (at lowest order) produce leptons that are back-to-back in transverse kinematics. Therefore, to take the effect

Contribution	$p_T^\ell > 4$ GeV	$p_T^\ell > 4$ GeV, $\lvert\eta^\ell\rvert < 2.4$, $m_{\ell^+\ell^-} > 10$ GeV
$\gamma_{\rm el}^p$	44.9(1) nb	17.5(1) nb
$\gamma_{\rm el}^p + \gamma_{\rm inel}^p$ [CT14qed_inc]	98.0(1) nb	39.7(1) nb
$\gamma_{\rm el}^p + \gamma_{\rm inel}^p$ [LUXqed17]	105.8(1) nb	44.1(1) nb
$\gamma_{\rm el}^p + \gamma_{\rm inel}^p$ [NNPDF3.1luxQED]	115.6(1) nb	45.9(1) nb
$\gamma_{\rm el}^p + \gamma_{\rm inel}^p$ [HKR16qed]	121.6(1) nb	49.4(1) nb

TABLE II: Integrated fiducial cross sections for $p + {\rm Pb} \to {\rm Pb} + \ell^+\ell^- + X$ production at $\sqrt{s_{NN}} = 8.16$ TeV for different collinear photon PDF sets. An effect of applying only p_T^ℓ requirement is shown in second column. For comparison, the cross section for purely elastic contribution is also shown.

contribution	$\sqrt{s}_{NN}$ = 8.16 TeV	$\sqrt{s}_{NN}$ = 8.16 TeV
	without cuts	$p_T > 4$ GeV, $\|y\| < 2.4$, $M_{l^+l^-} > 10$ GeV
LUX-like F2+FL		
$\gamma_{in}\gamma_{el}$	42.57	17.07
LUX-like F2		
$\gamma_{in}\gamma_{el}$	43.58	17.44
ALLM97 F2		
$\gamma_{in}\gamma_{el}$	41.72	16.43
Fiore et al.		
(parametrization of JLAB data)		
$\gamma_{in}\gamma_{el}$	45.24	18.36
SU F2		
$\gamma_{in}\gamma_{el}$	41.72	16.70
SY F2		
$\gamma_{in}\gamma_{el}$	40.38	15.99
Elastic- Elastic		
$\gamma_{el}\gamma_{el}$	47,89	18.26

TABLE III: Cross sections (in nb) for different contributions and different structure functions: LUX-like, ALLM97, Fiore, SU and SY. (the cross section was scaled by factors: 0.96 (elastic-elastic); 0.95 (elastic-inelastic) for proton-ion absorption (multiple interactions))

of inelastic photon virtuality into account, a dedicated parton shower algorithm should be used.

(mention we don't want to do extra PS; we would rather stick to kt factorization)

V. RESULTS INCLUDING PHOTON TRANSVERSE MOMENTUM

VI. DISCUSSION

We take the opportunity to calculate expected number of events for realistic assumption on total integrated luminosity. based on the previous pPb runs at the LHC, we assume $\int Ldt = 200$ nb^{-1}.

(show some table(s) here)

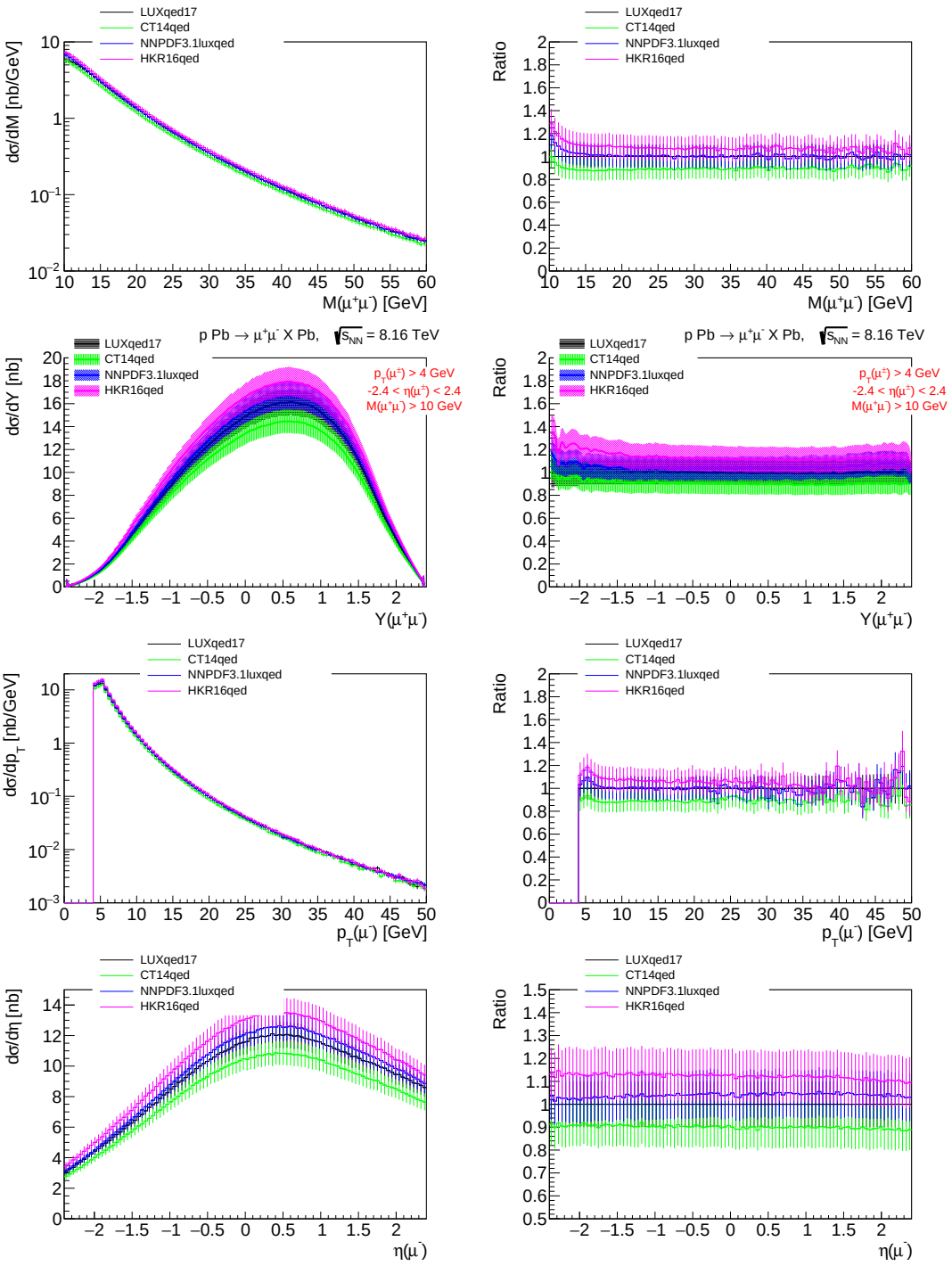

FIG. 2: Differential cross sections in the fiducial region for $p + \mathrm{Pb} \to \mathrm{Pb} + \ell^+\ell^- + X$ production at $\sqrt{s_{NN}} = 8.16$ TeV for different collinear photon PDF sets. Four differential distributions are shown (from top to bottom): invariant mass of lepton pair, pair rapidity, transverse momentum of negatively-charged lepton and its pseudorapidity. Figures on the right show the ratios to LUXqed17 PDF.

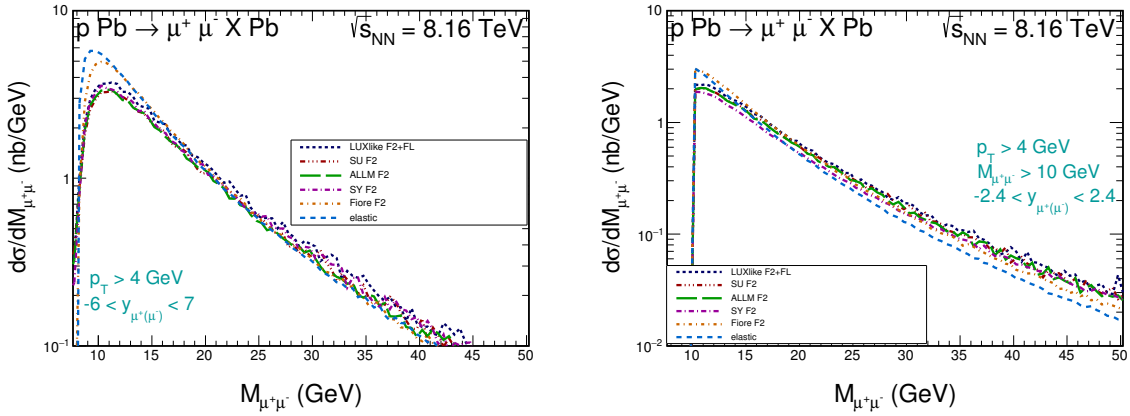

FIG. 3: The elastic - elastic and the inelastic-elastic contribution to dilepton invariant mass distributions for different structure functions. In the left panel we show the results for the whole phase space, while in the right panel only for the fiducial region.

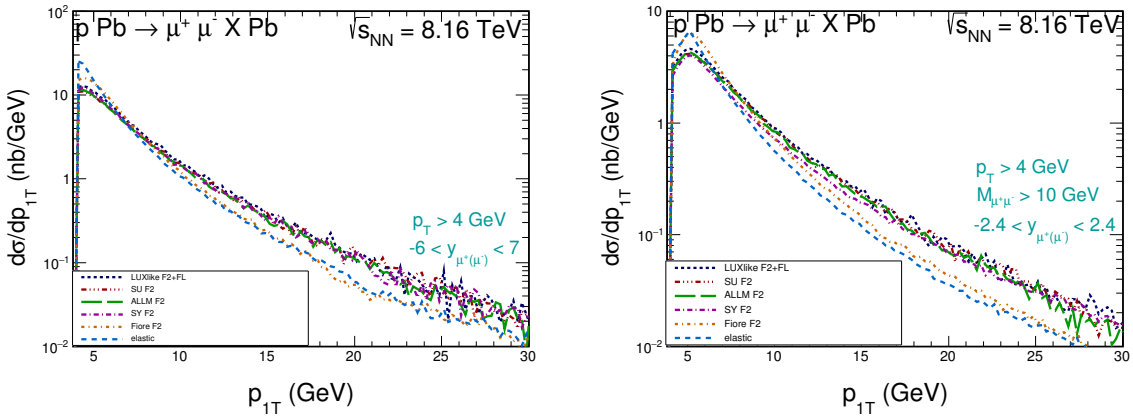

FIG. 4: Transverse momentum distribution of μ^+ or μ^- for elastic - elastic and inelastic - elastic different structure functions: LUX-like, ALLM97, Fiore at all., SU and SY (in the left panel we show the results for the whole phase space, while in the right panel only for the fiducial region).

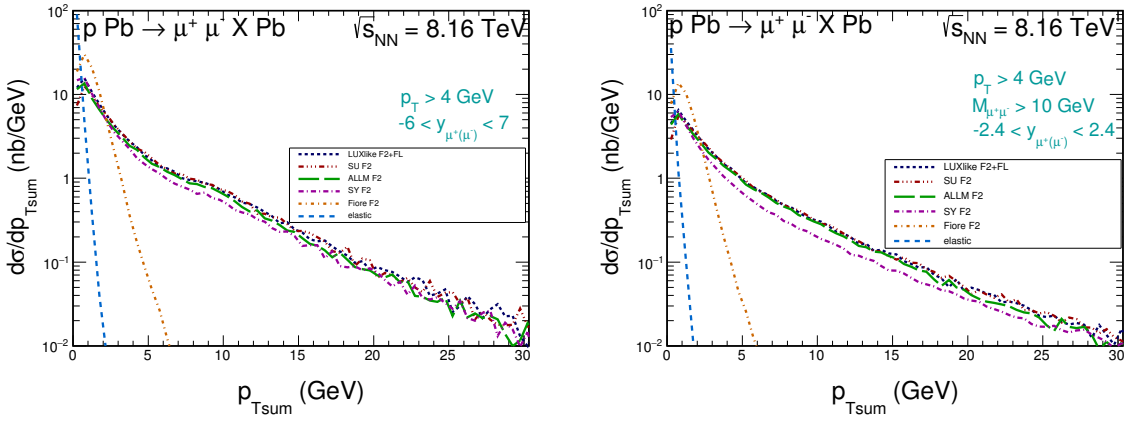

FIG. 5: Distribution in transverse momentum of the $\mu^+\mu^-$ pairs for elastic - elastic and inelastic-elastic contributions for different structure functions: LUX-like, ALLM97, Fiore at all., SU and SY. (in the left panel we show the results for the whole phase space, while in the right panel only for the fiducial region).

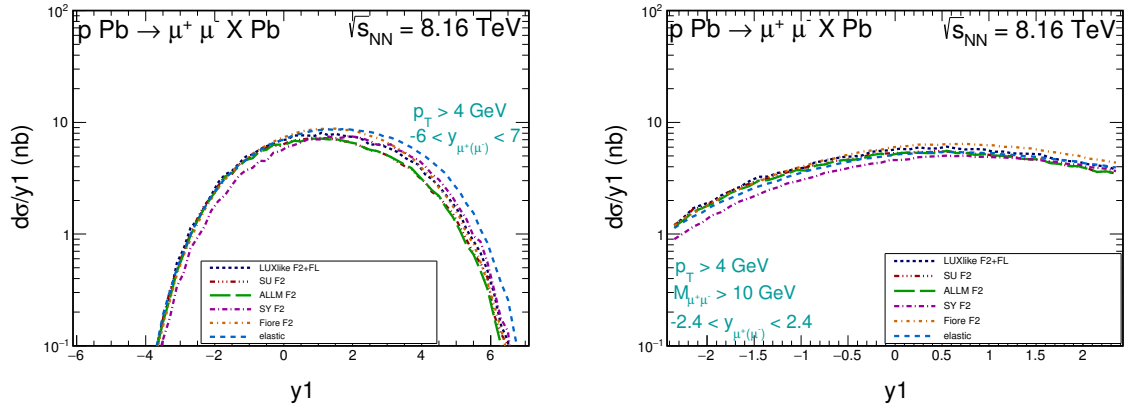

FIG. 6: Rapidity distribution of μ^+ or μ^- leptons for elastic - elastic and inelastic-elastic contributions for different structure functions: LUX-like, ALLM97, Fiore at all., SU and SY. (in the left panel we show the results for the whole phase space, while in the right panel only for the fiducial region).

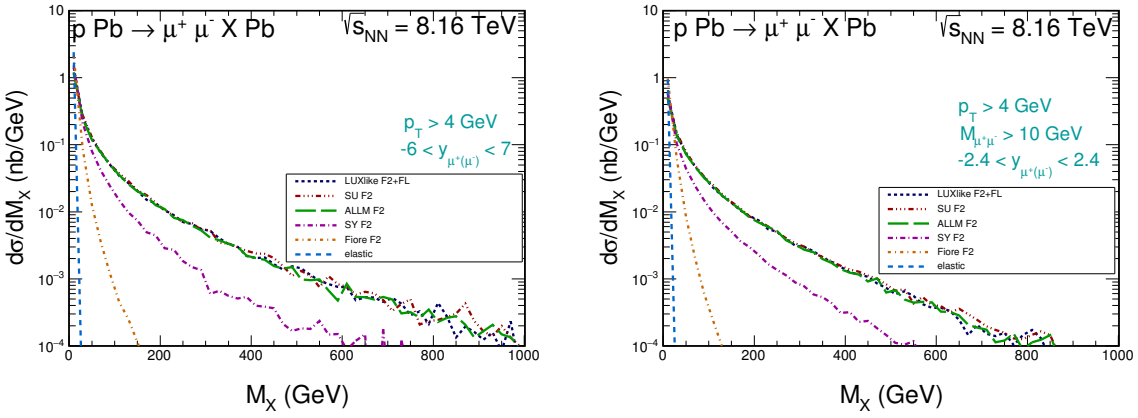

FIG. 7: Missing mass distributions for eleastic-elastic photon-photon contributions and elastic-inelastic photon-photon contributions for different structure functions: LUX-like, ALLM97, Fiore at all., SU and SY. (in the left panel we show the results for the whole phase space, while in the right panel only for the fiducial region).

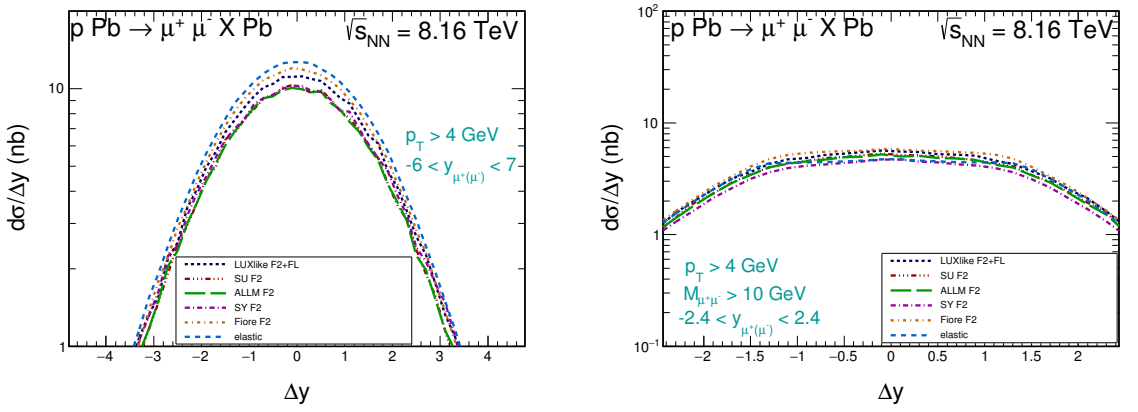

FIG. 8: Distribution in rapidity distance between $\mu^+\mu^-$ leptons. The calculation for the $\gamma - \gamma$ contribution was performed for different structure functions. The left panel shows results without cuts while the right panel shows results with ATLAS cuts.

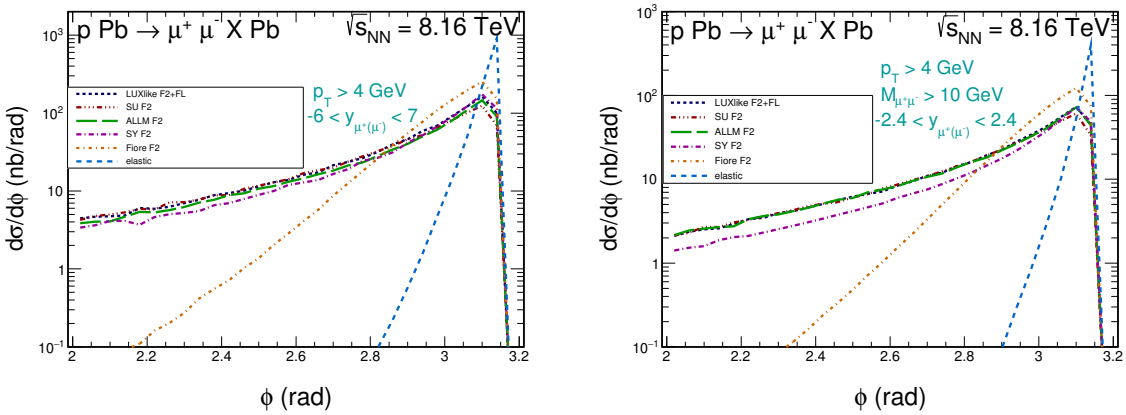

FIG. 9: Distributions for azimuthal angle between $\mu^+\mu^-$ leptons. (in the left panel we show the results for the whole phase space, while in the right panel only for the fiducial region).

VII. SUMMARY

In summary, we propose a method that would unambiguously allow to test and constrain the photon parton distribution at LHC energies.

References

[1] ATLAS Collaboration, G. Aad et al., *Measurement of the low-mass Drell-Yan differential cross section at $\sqrt{s}$ = 7 TeV using the ATLAS detector*, JHEP **06** (2014) 112, arXiv:1404.1212 [hep-ex].

[2] ATLAS Collaboration, G. Aad et al., *Measurement of the double-differential high-mass Drell-Yan cross section in pp collisions at $\sqrt{s} = 8$ TeV with the ATLAS detector*, JHEP **08** (2016) 009, arXiv:1606.01736 [hep-ex].

[3] E. Accomando, J. Fiaschi, F. Hautmann, S. Moretti, and C. H. Shepherd-Themistocleous, *Photon-initiated production of a dilepton final state at the LHC: Cross section versus forward-backward asymmetry studies*, Phys. Rev. **D95** (2017) no. 3, 035014, arXiv:1606.06646 [hep-ph].

[4] M. Luszczak, W. Schafer, and A. Szczurek, *Two-photon dilepton production in proton-proton collisions: two alternative approaches*, Phys. Rev. **D93** (2016) no. 7, 074018, arXiv:1510.00294 [hep-ph].

[5] L. A. Harland-Lang, V. A. Khoze, and M. G. Ryskin, *The photon PDF in events with rapidity gaps*, Eur. Phys. J. **C76** (2016) no. 5, 255, arXiv:1601.03772 [hep-ph].

[6] M. Luszczak, A. Szczurek, and C. Royon, *W^+W^- pair production in proton-proton collisions: small missing terms*, JHEP **02** (2015) 098, arXiv:1409.1803 [hep-ph].

[7] A. Denner, S. Dittmaier, M. Hecht, and C. Pasold, *NLO QCD and electroweak corrections to $Z + \gamma$ production with leptonic Z-boson decays*, JHEP **02** (2016) 057, arXiv:1510.08742 [hep-ph].

[8] M. Dyndal and L. Schoeffel, *Four-lepton production from photon-induced reactions in pp collisions at the LHC*, Acta Phys. Polon. **B47** (2016) 1645, arXiv:1511.02065 [hep-ph].

[9] M. Ababekri, S. Dulat, J. Isaacson, C. Schmidt, and C. P. Yuan, *Implication of CMS data on photon PDFs*, arXiv:1603.04874 [hep-ph].

[10] B. Biedermann, M. Billoni, A. Denner, S. Dittmaier, L. Hofer, B. Jger, and L. Salfelder, *Next-to-leading-order electroweak corrections to $pp \to W^+W^- \to 4$ leptons at the LHC*, JHEP **06** (2016) 065, arXiv:1605.03419 [hep-ph].

[11] B. Biedermann, A. Denner, S. Dittmaier, L. Hofer, and B. Jger, *Electroweak corrections to $pp \to \mu^+\mu^- e^+ e^- + X$ at the LHC: a Higgs background study*, Phys. Rev. Lett. **116** (2016) no. 16, 161803, arXiv:1601.07787 [hep-ph].

[12] Y. Wang, R.-Y. Zhang, W.-G. Ma, X.-Z. Li, and L. Guo, *QCD and electroweak corrections to ZZ+jet production with Z -boson leptonic decays at the LHC*, Phys. Rev. **D94** (2016) no. 1, 013011, arXiv:1604.04080 [hep-ph].

[13] M. Luszczak, W. Schafer, and A. Szczurek, *Production of W^+W^- pairs via $\gamma^*\gamma^* \to W^+W^-$ subprocess with photon transverse momenta*, JHEP **05** (2018) 064, arXiv:1802.03244 [hep-ph].

[14] A. Manohar, P. Nason, G. P. Salam, and G. Zanderighi, *How bright is the proton? A precise determination of the photon parton distribution function*, Phys. Rev. Lett. **117** (2016) no. 24, 242002, arXiv:1607.04266 [hep-ph].

[15] C. Schmidt, J. Pumplin, D. Stump, and C. P. Yuan, *CT14QED parton distribution functions from isolated photon production in deep inelastic scattering*, Phys. Rev. **D93** (2016) no. 11, 114015, arXiv:1509.02905 [hep-ph].

[16] NNPDF Collaboration, R. D. Ball, V. Bertone, S. Carrazza, L. Del Debbio, S. Forte, A. Guffanti, N. P. Hartland, and J. Rojo, *Parton distributions with QED corrections*, Nucl. Phys. **B877** (2013) 290–320, arXiv:1308.0598 [hep-ph].

[17] xFitter Developers' Team Collaboration, F. Giuli et al., *The photon PDF from high-mass Drell-Yan data at the LHC*, Eur. Phys. J. **C77** (2017) no. 6, 400, arXiv:1701.08553 [hep-ph].

[18] ATLAS Collaboration, G. Aad et al., *Measurement of exclusive $\gamma\gamma \to \ell^+\ell^-$ production in proton-proton collisions at $\sqrt{s} = 7$ TeV with the ATLAS detector*, Phys. Lett. **B749** (2015) 242–261, arXiv:1506.07098 [hep-ex].

[19] ATLAS Collaboration, M. Aaboud et al., *Measurement of the exclusive $\gamma\gamma \to \mu^+\mu^-$ process in proton-proton collisions at $\sqrt{s} = 13$ TeV with the ATLAS detector*, Phys. Lett. **B777**

(2018) 303–323, arXiv:1708.04053 [hep-ex].

[20] CMS Collaboration, S. Chatrchyan et al., *Exclusive photon-photon production of muon pairs in proton-proton collisions at* $\sqrt{s} = 7\ TeV$, JHEP **01** (2012) 052, arXiv:1111.5536 [hep-ex].

[21] CMS Collaboration, S. Chatrchyan et al., *Search for exclusive or semi-exclusive photon pair production and observation of exclusive and semi-exclusive electron pair production in pp collisions at* $\sqrt{s} = 7\ TeV$, JHEP **11** (2012) 080, arXiv:1209.1666 [hep-ex].

[22] CMS, TOTEM Collaboration, A. M. Sirunyan et al., *Observation of proton-tagged, central (semi)exclusive production of high-mass lepton pairs in pp collisions at 13 TeV with the CMS-TOTEM precision proton spectrometer*, JHEP **07** (2018) 153, arXiv:1803.04496 [hep-ex].

[23] V. M. Budnev, I. F. Ginzburg, G. V. Meledin, and V. G. Serbo, *The two photon particle production mechanism. Physical problems. Applications. Equivalent photon approximation*, Phys. Rept. **15** (1975) 181.

[24] S. R. Klein, J. Nystrand, J. Seger, Y. Gorbunov, and J. Butterworth, *STARlight: A Monte Carlo simulation program for ultra-peripheral collisions of relativistic ions*, Comput. Phys. Commun. **212** (2017) 258–268, arXiv:1607.03838 [hep-ph].

[25] M. Gluck, C. Pisano, and E. Reya, *The Polarized and unpolarized photon content of the nucleon*, Phys. Lett. **B540** (2002) 75–80, arXiv:hep-ph/0206126 [hep-ph].

[26] A. D. Martin, R. G. Roberts, W. J. Stirling, and R. S. Thorne, *Parton distributions incorporating QED contributions*, Eur. Phys. J. **C39** (2005) 155–161, arXiv:hep-ph/0411040 [hep-ph].

[27] A. D. Martin and M. G. Ryskin, *The photon PDF of the proton*, Eur. Phys. J. **C74** (2014) 3040, arXiv:1406.2118 [hep-ph].

[28] C. Schmidt, J. Pumplin, D. Stump, and C. P. Yuan, *QED effects and Photon PDF in the CTEQ-TEA Global Analysis*, PoS **DIS2014** (2014) 054.

[29] L. A. Harland-Lang, V. A. Khoze, and M. G. Ryskin, *Photon-initiated processes at high mass*, Phys. Rev. **D94** (2016) no. 7, 074008, arXiv:1607.04635 [hep-ph].

[30] NNPDF Collaboration, V. Bertone, S. Carrazza, N. P. Hartland, and J. Rojo, *Illuminating the photon content of the proton within a global PDF analysis*, SciPost Phys. **5** (2018) 008, arXiv:1712.07053 [hep-ph].

[31] G. G. da Silveira, L. Forthomme, K. Piotrzkowski, W. Schfer, and A. Szczurek, *Central production via photon-photon fusion in proton-proton collisions with proton dissociation*, JHEP **02** (2015) 159, arXiv:1409.1541 [hep-ph].

[32] H. Abramowicz, E. M. Levin, A. Levy, and U. Maor, *A Parametrization of sigma-T (gamma* p) above the resonance region $Q^2 \geq 0$*, Phys. Lett. **B269** (1991) 465–476.

[33] H. Abramowicz and A. Levy, *The ALLM parameterization of sigma(tot)(gamma* p): An Update*, arXiv:hep-ph/9712415 [hep-ph].

[34] R. Fiore, A. Flachi, L. L. Jenkovszky, A. I. Lengyel, and V. K. Magas, *Explicit model realizing parton hadron duality*, Eur. Phys. J. **A15** (2002) 505–515, arXiv:hep-ph/0206027 [hep-ph].

[35] A. Suri and D. R. Yennie, *THE SPACE-TIME PHENOMENOLOGY OF PHOTON ABSORPTION AND INELASTIC ELECTRON SCATTERING*, Annals Phys. **72** (1972) 243.

[36] A. Szczurek and V. Uleshchenko, *Nonpartonic components in the nucleon structure functions at small Q^2 in the broad range of x*, Eur. Phys. J. **C12** (2000) 663–671, arXiv:hep-ph/9904288 [hep-ph].

[37] P. E. Bosted and M. E. Christy, *Empirical fit to inelastic electron-deuteron and electron-neutron resonance region transverse cross-sections*, Phys. Rev. **C77** (2008) 065206, arXiv:0711.0159 [hep-ph].

[38] HERMES Collaboration, A. Airapetian et al., *Inclusive Measurements of Inelastic Electron and Positron Scattering from Unpolarized Hydrogen and Deuterium Targets*, JHEP **05** (2011) 126, arXiv:1103.5704 [hep-ex].

[39] E143 Collaboration, K. Abe et al., *Measurements of $R = \sigma(L) / \sigma(T)$ for $0.03 < x < 0.1$ and fit to world data*, Phys. Lett. **B452** (1999) 194–200, arXiv:hep-ex/9808028 [hep-ex].

[40] A. V. Manohar, P. Nason, G. P. Salam, and G. Zanderighi, *The Photon Content of the Proton*, JHEP **12** (2017) 046, arXiv:1708.01256 [hep-ph].

[41] ATLAS Collaboration, G. Aad et al., *The ATLAS Experiment at the CERN Large Hadron Collider*, JINST **3** (2008) S08003.

[42] CMS Collaboration, S. Chatrchyan et al., *The CMS Experiment at the CERN LHC*, JINST **3** (2008) S08004.

[43] S. D. Drell and T.-M. Yan, *Massive Lepton Pair Production in Hadron-Hadron Collisions at*

High-Energies, Phys. Rev. Lett. **25** (1970) 316–320. [Erratum: Phys. Rev. Lett.25,902(1970)].

[44] ATLAS Collaboration, G. Aad et al., *Z boson production in p+Pb collisions at* $\sqrt{s_{NN}} = 5.02$ *TeV measured with the ATLAS detector*, Phys. Rev. **C92** (2015) no. 4, 044915, arXiv:1507.06232 [hep-ex].

[45] CMS Collaboration, V. Khachatryan et al., *Study of Z boson production in pPb collisions at* $\sqrt{s_{NN}} = 5.02$ *TeV*, Phys. Lett. **B759** (2016) 36–57, arXiv:1512.06461 [hep-ex].

[46] ALICE Collaboration, J. Adam et al., *W and Z boson production in p-Pb collisions at* $\sqrt{s_{\rm NN}}$ *= 5.02 TeV*, JHEP **02** (2017) 077, arXiv:1611.03002 [nucl-ex].

[47] ALICE Collaboration, G. Dellacasa et al., *ALICE technical design report of the zero degree calorimeter (ZDC)*, . CERN-LHCC-99-05.

[48] ATLAS Collaboration, *Zero degree calorimeters for ATLAS*, . CERN-LHCC-2007-01.